

Monogamy of quantum correlations reveals frustration in a quantum Ising spin system: Experimental demonstration

K. Rama Koteswara Rao¹, Hemant Katiyar², T. S. Mahesh², Aditi Sen(De)³, Ujjwal Sen³, and Anil Kumar¹

¹*Centre for Quantum Information and Quantum Computation,*

*Department of Physics and NMR Research Centre,
Indian Institute of Science, Bangalore 560012, India*

²*Department of Physics and NMR Research Center,*

Indian Institute of Science Education and Research, Pune 411008, India

³*Harish-Chandra Research Institute, Chhatnag Road, Jhansi, Allahabad 211 019, India*

We report a nuclear magnetic resonance experiment, which simulates the quantum transverse Ising spin system in a triangular configuration and further show that the monogamy of quantum correlations can be used to distinguish between the frustrated and non-frustrated regimes in the ground state of this system. Adiabatic state preparation methods are used to prepare the ground states of the spin system. We employ two different multipartite quantum correlation measures to analyze the experimental ground state of the system in both the frustrated and non-frustrated regimes. In particular, we use multipartite quantum correlation measures generated by monogamy considerations of negativity, a bipartite entanglement measure, and that of quantum discord, an information-theoretic quantum correlation measure. As expected from theoretical predictions, the experimental data confirm that the non-frustrated regime shows higher multipartite quantum correlations compared to the frustrated one.

PACS numbers: 03.67.-a, 03.67.Mn, 75.10.Jm, 82.56.-b

I. INTRODUCTION

Recently, quantum correlations [1, 2] have been employed beyond its traditional ambit of quantum computation and information, and used as tools in quantum many-body physics [2–4]. Detecting phases of many-body systems is an important task with fundamental as well as technological implications [5]. Frustrated cooperative phenomena form one of the centerstages of the research in many-body physics. Frustration in a many-body Hamiltonian appears when it is not possible to simultaneously minimize each of the energy bonds in the Hamiltonian independently, and may appear as a result of competing interactions due to the geometry of the lattice or due to incommensurate values of the coupling strengths [6]. Frustrated systems usually possess hugely degenerate ground states and a rich phase diagram ranging from quantum spin liquids to resonating valence-bond states [7]. Very recently, theoretical studies have shown that entanglement can be an effective tool for investigating frustrated quantum systems [8, 9]. Frustrated interactions had been known to be present in several solid state systems [7]. Recent experimental breakthroughs have made it possible to engineer frustrated spin models in ultracold atoms in optical lattices [10], trapped ions [11], NMR [12], etc, and have led to the possibility of observing the effects of entanglement in the different phases of frustrated spin models in the laboratory.

In the present work, we employ multipartite quantum correlations to distinguish the frustrated regimes from the non-frustrated ones. There are many ways by which multipartite quantum correlations can be quantified [1, 2] and even though their properties can vary widely, there are some distinct connecting themes. One of them is the

“monogamy” of bipartite quantum correlations, which broadly demands that if two parties are strongly quantum correlated, they cannot have a significant amount of the same with a third party [13–15].

There is a two-fold aim of the present work. First of all, we want to experimentally observe the effect of monogamy of bipartite quantum correlations in a multiparty quantum system. Secondly, we wish to apply the concept of monogamy of such correlations to distinguish between frustrated and non-frustrated regimes in a quantum Ising spin system. To attain our goal, we prepare a transverse Ising spin system [16] in a triangular configuration by using NMR techniques. It undergoes a transition from a non-frustrated regime to a frustrated one when its coupling strength is varied from a ferromagnetic to an antiferromagnetic regime. We study the multipartite quantum correlations of the ground state to detect the two different regimes. Specifically, we consider multiparty quantum correlation measures, generated from monogamy studies of bipartite quantum correlations [13–15]. In analyzing the experimentally generated ground state, we employ monogamy of (i) negativity [15, 17, 18], which is a bipartite entanglement measure, and of (ii) quantum discord [19, 20], which is an information-theoretic quantum correlation measure. For such investigations, we initially prepare the spin system in the ground state of the transverse field Hamiltonian, which is a product state and then adiabatically drive it to both frustrated and non-frustrated regimes in such a way that the system remains in the ground state of the instantaneous Hamiltonian. We then calculate the multipartite correlations of the ground state by performing quantum state tomography at different time intervals. Moreover, coinciding with the theoretical sim-

ulations, we observe that the non-frustrated regime has higher multipartite quantum correlations than the frustrated one. The transition point from the non-frustrated to the frustrated regime is well indicated by the vanishing monogamy relation.

The paper is arranged as follows. In Sec. II, we present the multipartite quantum correlations that are employed in analyzing the ground state. We describe the frustrated and non-frustrated quantum Ising spin systems in Sec. III. The experimental results are presented in Sec. IV and we conclude in Sec. V.

II. MULTIPARTITE QUANTUM CORRELATIONS

Quantum correlations of a multipartite quantum state can be quantified in a variety of approaches. A prominent one among them is to use the concept of monogamy of bipartite quantum correlations [15, 17, 20]. In a tripartite scenario, monogamy of a bipartite quantum correlation restricts the amount of that correlation which can be shared between the three parties. Let us suppose that three parties, Alice, Bob, and Charu, denoted respectively as 1, 2, and 3, share a tripartite quantum state. Monogamy of quantum correlations implies that if 1 has substantial quantum correlations with 2, it can have only a restricted amount of the same with 3. To state it more precisely, for a bipartite quantum correlation measure \mathcal{Q} and a tripartite quantum state ρ_{123} , one can introduce a quantity, known as “monogamy score for \mathcal{Q} ” [21] and denote as $\delta_{\mathcal{Q}}$, given by

$$\delta_{\mathcal{Q}}(\rho_{123}) = \mathcal{Q}_{1(23)} - \mathcal{Q}_{12} - \mathcal{Q}_{13}, \quad (1)$$

where $\mathcal{Q}_{1(23)}$ is the bipartite quantum correlation measured for the state ρ_{123} in the 1 : 23 partition. \mathcal{Q}_{12} is the same measure for the reduced state $\rho_{12} = \text{tr}_3 \rho_{123}$, and similarly for \mathcal{Q}_{13} . The three-party quantum state ρ_{123} is said to be monogamous with respect to the bipartite quantum correlation measure \mathcal{Q} , if $\delta_{\mathcal{Q}}(\rho_{123}) \geq 0$. A measure for which all tripartite quantum states produce non-negative monogamy scores is said to be “monogamous”.

The monogamy score, and its properties, will certainly depend on the bipartite quantum correlation measure that is employed to define the score. There are many ways in which one can conceptualize bipartite quantum correlations, and correspondingly there are many bipartite quantum correlation measures [1, 2]. Broadly, these measures are defined within two paradigms, viz. the entanglement-separability paradigm and the information-theoretic one. We consider bipartite quantum correlation measures from both these paradigms to define monogamy scores, that are subsequently used for distinguishing frustrated regimes of quantum spin systems from non-frustrated ones in the experiment. As we will see below, one of these measures is

monogamous for pure three-qubit quantum states, while the other is not.

Monogamy Score for Negativity Squared. – Negativity is an important quantum correlation measure for two-party quantum states [18]. It is defined within the entanglement-separability paradigm. The negativity, N_{12} , of an arbitrary bipartite quantum state ρ_{12} is the absolute value of the sum of the negative eigenvalues of the partial transposed state $\rho_{12}^{T_1}$, where the partial transposition is taken with respect to Alice (1). The importance of this measure arises from the fact that if a partially transposed bipartite quantum state has negative eigenvalues, the state must be entangled [22].

Replacing \mathcal{Q} in Eq. (1) by the squared negativity, we obtain the monogamy score for the negativity squared, given by

$$\delta_{N^2} = N_{1(23)}^2 - N_{12}^2 - N_{13}^2. \quad (2)$$

Recently, it has been shown that the negativity squared is monogamous, i.e. $\delta_{N^2} \geq 0$, for all three-qubit pure states [17]. In this paper, we measure δ_{N^2} in both the frustrated and non-frustrated regimes. For ease of reference, we call the monogamy score for negativity squared as the “entanglement monogamy score”.

Quantum Discord and Monogamy. – Let us now define another bipartite measure of quantum correlation, and importantly it does not belong to the entanglement-separability paradigm. Quantum discord is defined as the difference between two classically equivalent formulations of mutual information, when the systems involved are quantum [19], and is given by

$$D_{12} = D(\rho_{12}) = I(\rho_{12}) - J(\rho_{12}), \quad (3)$$

where $I(\rho_{12})$ and $J(\rho_{12})$ are argued to be, respectively, measures of total and classical correlations of ρ_{12} . $I(\rho_{12})$ is defined as $S(\rho_1) + S(\rho_2) - S(\rho_{12})$, where $S(\sigma) = -\text{tr}(\sigma \log_2 \sigma)$ is the von Neumann entropy of σ , $\rho_1 = \text{tr}_2 \rho_{12}$, and $\rho_2 = \text{tr}_1 \rho_{12}$. $J(\rho_{12}) = S(\rho_2) - S(\rho_{2|1})$, where the conditional entropy $S(\rho_{2|1}) = \min_{\Pi_1^1} \sum_i p_i S(\rho_{2|\Pi_1^1})$, with the minimization being performed over all possible rank-one projection-valued measurements Π_1^1 on subsystem 1. Here the output state $\rho_{2|\Pi_1^1} = \Pi_1^1 \rho_{12} \Pi_1^1 / \text{tr}_{12}(\Pi_1^1 \rho_{12})$, and the probability $p_i = \text{Tr}(\Pi_1^1 \rho_{12})$. The monogamy score for quantum discord (referred later as the “discord monogamy score”) for a tripartite state ρ_{123} is given by [20]

$$\delta_D = D_{1(23)} - D_{12} - D_{13}. \quad (4)$$

Unlike the entanglement monogamy score, the discord monogamy score, δ_D , can be both nonnegative and negative, even for pure tripartite states [20].

III. FRUSTRATED ISING SPIN SYSTEM

Frustrated spin systems have attracted a lot of interest due to their rich phase diagrams. Frustration can

be observed in a system consisting of three quantum spin-1/2 particles positioned at the corners of an equilateral triangle, and having Ising (nearest-neighbor) interactions. The Hamiltonian of this three-spin transverse Ising model is given by

$$\mathcal{H} = h(\sigma_x^1 + \sigma_x^2 + \sigma_x^3) + J(\sigma_z^1\sigma_z^2 + \sigma_z^2\sigma_z^3 + \sigma_z^1\sigma_z^3), \quad (5)$$

where h is the strength of the transverse field, J is the coupling strength of the Ising interactions, and $|J| \gg h$. The three quantum spin-1/2 particles are denoted as 1, 2, 3. σ_x^i and σ_z^i , for $i = 1, 2, 3$, are the Pauli spin matrices at site i . When $J > 0$, i.e., the Ising interactions are of anti-ferromagnetic type, the system is frustrated, whereas when $J < 0$, i.e., the Ising interactions are of ferromagnetic type, the system is non-frustrated.

We now describe the adiabatic state preparation method used to prepare the ground state of this spin system in the laboratory [23]. The quantum adiabatic theorem states that if a system is initially in the ground state and if its Hamiltonian evolves slowly with time, it will be found at any later time in the ground state of the instantaneous Hamiltonian [24]. The Hamiltonian evolution rate is governed by the relation

$$\frac{|\langle 1; t | \frac{d\mathcal{H}(t)}{dt} | 0; t \rangle|}{g^2(t)} \leq \epsilon, \quad (6)$$

where ϵ is a small number, $|0; t\rangle$ and $|1; t\rangle$ are respectively the ground and first excited states of the instantaneous Hamiltonian $\mathcal{H}(t)$, and $g(t)$ is the energy difference between the corresponding energy levels. The system stays in the instantaneous ground state of the Hamiltonian with a probability $(1 - \epsilon^2)^2$.

The spin system is initially prepared in the ground state of the Hamiltonian $h(\sigma_x^1 + \sigma_x^2 + \sigma_x^3)$. Then the system is taken to the frustrated regime by adiabatically increasing J from 0 to $|J_{max}|$ and similarly to the non-frustrated regime by decreasing J from 0 to $-|J_{max}|$, where $|J_{max}| \gg h$. The system stays in the ground state of the instantaneous Hamiltonian with high probability, if J is changed slowly enough so that it satisfies Eq. (6). The energy level diagram of the spin system is shown in the Fig. 1. The energy level of the ground state of the system is represented by the solid red curve, which is marked as E_0 . The energy level of the only excited state which is relevant in the calculation of the adiabatic evolution rate of the Hamiltonian is represented by the other solid red curve, which is marked as E_1 . The energy levels of all the other excited states are shown by blue dashed curves. Though there are energy levels in between E_0 and E_1 , there are no possible transitions from the ground state to these excited states, as the transition amplitudes (given by the matrix elements similar to the numerator of the left hand side in Eq. (6)) are zero in these cases.

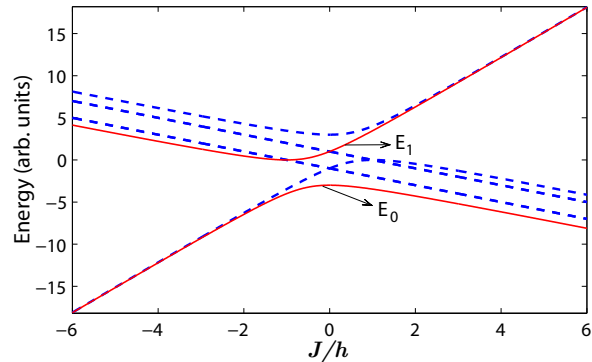


FIG. 1. Energy level diagram. The red solid curves, which are marked as E_0 and E_1 , represent respectively the energy levels of the ground state and the excited state which is relevant in the calculation of the adiabatic evolution rate (Eq. (6)). The blue dashed curves represent the energy levels corresponding to the other excited states.

IV. EXPERIMENTAL IMPLEMENTATION

The spin-system chosen for the experiments is iodotri-fluoroethylene (C_2F_3I) dissolved in acetone- D_6 . Here the three ^{19}F nuclear spins act as three spin-1/2 particles. The chemical structure of the molecule, the chemical shifts of the three fluorine nuclei, and the J -couplings between them are shown in Fig. 2. The experiments have been carried out at a temperature of 290 K in an 11.7 Tesla magnetic field on a Bruker UltraShield AV III 500 MHz NMR spectrometer using a QXI probe. The ^{19}F resonance frequency at this field is 470 MHz. The measured longitudinal relaxation time constants (T_1) of the three fluorine nuclei F_1 , F_2 , and F_3 are 6.9 s, 7.5 s, and 6.2 s respectively. The transverse relaxation time constants (T_2) of these nuclei, measured by Hahn echo, are 2.8 s, 3.1 s, and 3.3 s respectively.

In the rotating frame, the NMR Hamiltonian of a weakly coupled three-spin system is given by

$$\mathcal{H}_{\text{NMR}} = - \sum_{i=1}^3 \pi \nu_i \sigma_z^i + \sum_{i < j, =1}^3 \frac{\pi}{2} J_{ij} \sigma_z^i \sigma_z^j. \quad (7)$$

where ν_i are the chemical shifts of the ^{19}F nuclear spins, J_{ij} are the scalar coupling constants between them. The equilibrium density matrix under high temperature and high field approximation, is in a highly mixed state, given by

$$\rho_{eq} = \frac{1}{8}(I + \zeta \Delta \rho_{eq}), \quad (8)$$

where $\zeta \sim 10^{-5}$ is the purity factor and the deviation part of the density matrix [25]

$$\Delta \rho_{eq} \propto \sigma_z^1 + \sigma_z^2 + \sigma_z^3. \quad (9)$$

In liquid state room temperature NMR, since the preparation of a pure state requires extreme conditions, it is a

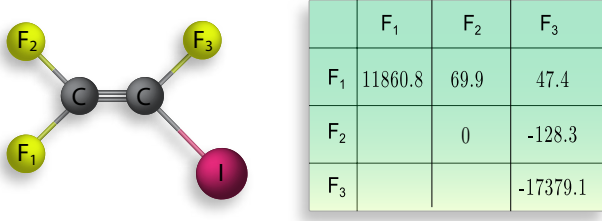


FIG. 2. Chemical structure of the molecule (left) and the table of Hamiltonian parameters (right). In the table, the diagonal elements are the chemical shifts ν_i (in Hz) of the fluorine spins and the off-diagonal elements are the scalar coupling constants J_{ij} (in Hz) between them.

common practice to prepare a pseudo-pure state (PPS) that mimics the pure state [26, 27]. We have used the spatial averaging method to prepare the $|000\rangle$ PPS from the equilibrium [26]. The total time taken to prepare this PPS is ≈ 30 ms.

In the experimental implementation, the Hamiltonian $\mathcal{H}(t)$ is discretized into $M+1$ steps as $\mathcal{H}(\frac{m}{M}T)$, where T is the total duration of the adiabatic evolution and m goes from 0 to M . The unitary operator corresponding to the each step is given by

$$U_m = \exp(-i\mathcal{H}(\frac{m}{M}T)\Delta t) = \exp(-i[h(\sigma_x^1 + \sigma_x^2 + \sigma_x^3) + J(\frac{m}{M}T)(\sigma_z^1\sigma_z^2 + \sigma_z^2\sigma_z^3 + \sigma_z^1\sigma_z^3)]\Delta t), \quad (10)$$

where $\Delta t = \frac{T}{M+1}$. The unitary operator corresponding to the total adiabatic evolution after the $(M+1)$ th step can be written as

$$U = \prod_{m=0}^M U_m. \quad (11)$$

The unitary operator for each step can be approximated to second order in Δt by using the Trotter's formula

$$U_m \approx \exp(-ih(\sigma_x^1 + \sigma_x^2 + \sigma_x^3)\frac{\Delta t}{2}) \times \exp(-iJ(\frac{m}{M}T)(\sigma_z^1\sigma_z^2 + \sigma_z^2\sigma_z^3 + \sigma_z^1\sigma_z^3)\Delta t) \times \exp(-ih(\sigma_x^1 + \sigma_x^2 + \sigma_x^3)\frac{\Delta t}{2}). \quad (12)$$

In the experiment, the value of $h\Delta t$ was set to $\pi/21$ and that of $J(T)\Delta t$ to $\pi/4$ and $-\pi/4$ in the frustrated and non-frustrated cases respectively. The value of $\frac{m}{M}$ was increased from 0 to 1 in 21 steps, in both the frustrated and non-frustrated cases. Considering the energy gap between the ground state (E_0) and the relevant excited state (E_1), increasing $J(t)$ linearly is not time-efficient. To achieve a time-efficient adiabatic evolution, we used a sine hyperbolic variation in $J(t)$. By using experimental parameters, we have estimated ϵ from the adiabatic relation of Eq. (6) and its maximum value is 0.063. This corresponds to a minimum probability of 0.992 for the system to stay in the ground state.

The ground state of the Hamiltonian at time $t = 0$, i.e. of $h(\sigma_x^1 + \sigma_x^2 + \sigma_x^3)$, is $|---\rangle$ with $|-\rangle = \frac{1}{\sqrt{2}}(|0\rangle - |1\rangle)$. This state was prepared from the $|000\rangle$ PPS by applying a $\frac{\pi}{2}$ rotation with respect to the $-y$ axis on all the three spins. This rotation was realized by a numerically optimized amplitude and phase modulated radio frequency (RF) pulse using Gradient Ascent Pulse Engineering (GRAPE) technique [28, 29]. The length of this pulse is 600 μ s.

The J -couplings of the spin system are unequal and constant, which cannot be changed directly. However, with judicious use of RF pulses one can create the effective Hamiltonians to simulate the adiabatic evolution of Eqs. (11) and (12). Here, we created these effective Hamiltonians by modulating the amplitude and phase of the RF pulses using GRAPE algorithm. As evident from Eq. (11), the adiabatic evolution after the k^{th} step can be written as a product of k unitary operators (U_k s) acting on the initial state. For efficient implementation of the adiabatic evolution, we generated GRAPE pulses by cascading these unitary operators. For example, in the 5th step, the unitary operator $U = U_4U_3U_2U_1U_0$ was realized by a single GRAPE pulse and applied on the initial state $|---\rangle$. This way we generated different GRAPE pulses for the combined unitary operators of the steps 3, 5, 7, \dots , 21 and applied on the initial state in both the regimes. The length of the pulses, which were used to realize the full adiabatic evolution (for 21 steps) in both the regimes, is 30 ms. The length of the pulses for realizing all the intermediate steps ranged between 1 ms to 30 ms. All the GRAPE pulses were optimized such that they are robust against RF field inhomogeneity and the average Hilbert-Schmidt fidelity of all these pulses are greater than 0.995. Quantum state tomography of the full density matrix was performed after the steps 3, 5, 7, \dots , 21 in both the frustrated and non-frustrated regimes. The reconstruction of the full density matrix involves an optimized set of 7 experiments and fitting of the corresponding real and imaginary parts of the single quantum spectra of all the three ^{19}F nuclear spins [30]. The real part of the reconstructed density matrices corresponding to the initial state $|---\rangle\langle---|$ and that of the final states corresponding to the last step in both the regimes are shown in the Fig. 3.

To quantitatively evaluate the experimental results, we calculate the fidelity (F) of the experimental density matrices (ρ_{exp}) with respect to the theoretical density matrices (ρ_{th}), given by

$$F = \frac{\text{tr}(\rho_{\text{th}}\rho_{\text{exp}})}{\sqrt{\text{tr}(\rho_{\text{th}}^2)\text{tr}(\rho_{\text{exp}}^2)}}. \quad (13)$$

The fidelity of the initial state $|---\rangle\langle---|$ was found to be 0.99 and that of all other final density matrices were greater than 0.984.

The entanglement and discord monogamy scores were calculated by using the relations in Eq. (2) and Eq. (4) respectively. We make an important change in our proce-

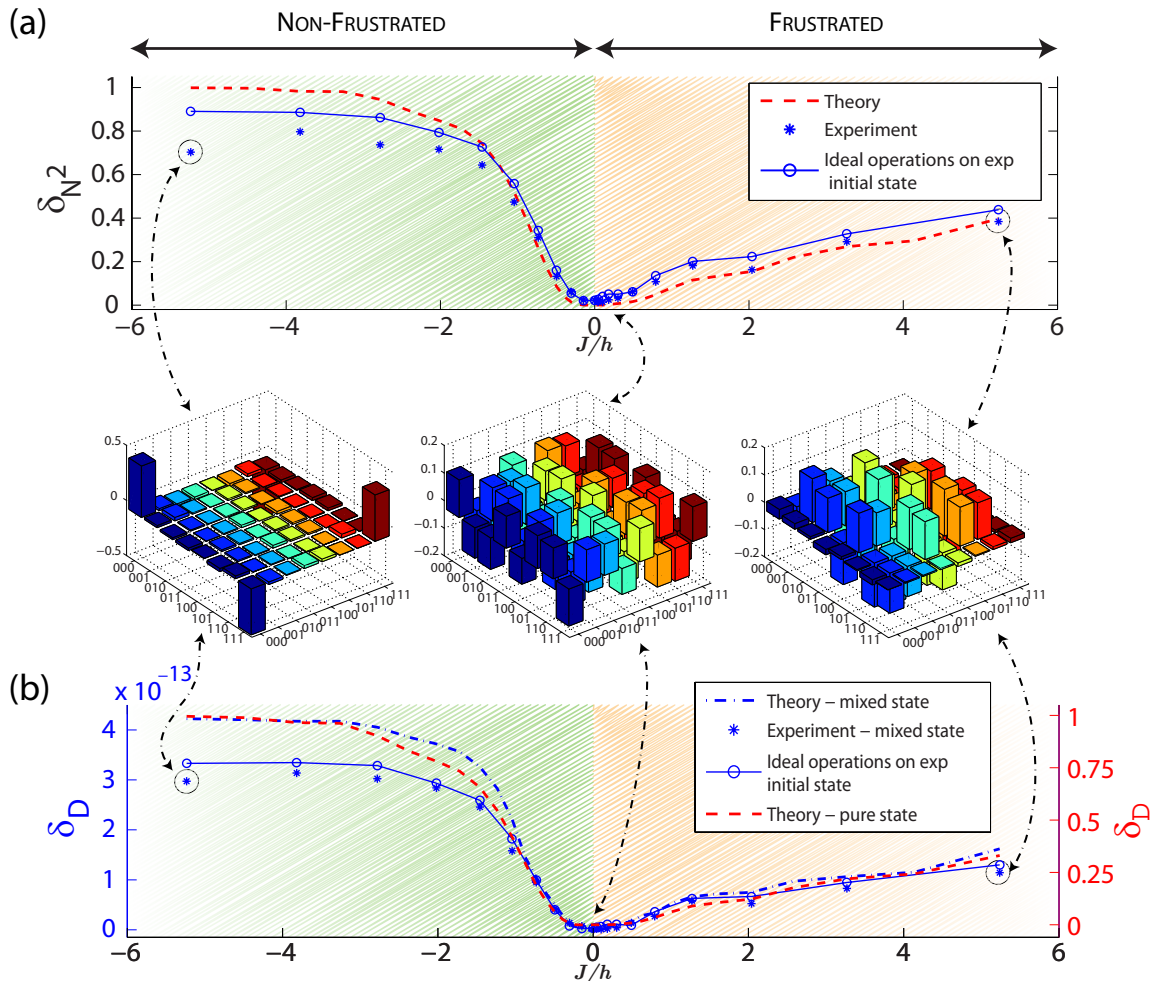


FIG. 3. (a) Entanglement and (b) Discord monogamy scores. The red-dashed curves correspond to the theoretically expected results, obtained by applying ideal unitary operations on the ideal initial state. The blue circles are obtained by applying the ideal unitary operations on the experimental initial state. The blue stars correspond to experimental results. In (b) the blue-dash-dotted curves correspond to the theoretically expected results for the mixed states of the NMR system, and the y-axis for the red-dashed curve is given at the right. For simulating all the theoretically expected density matrices, we used the Trotter's approximation of Eq. (12) and fixed the total number of steps for the adiabatic evolution as 21 for each, in both the regimes. The real parts of the experimental density matrices are also shown for the initial state $|---\rangle\langle---|$ (middle one), the final state in the non-frustrated regime (left one), and the final state in the frustrated regime (right one).

cedure to calculate the quantum discord of the experimental states. Instead of using only the pseudo-pure part of the experimental density matrix, as was done for calculating the negativity, we used the full mixed state density matrix of the NMR system for calculating the quantum discord. It is well known that the room temperature liquid-state NMR systems can have non-zero discord, although the purity of these systems is too small to exhibit any real entanglement [31, 32]. The negativity N_{12} and the quantum discord D_{12} measured from the experimental states along with the theoretically expected ones are given in the Appendix.

The experimental results along with the theoretically expected ones for entanglement monogamy score and that for discord monogamy score are shown in Fig. 3(a) and Fig. 3(b) respectively. It is clear from these results that the non-frustrated regime has higher multipartite quantum correlations compared to the frustrated one. In the case of discord monogamy score (Fig. 3(b)), the theoretically expected results are shown for both the pure (dashed red curve) and the NMR mixed state (dash-dotted blue curve) density matrices, where the latter's pseudo-pure part is proportional to the former. Although the discord monogamy scores of the mixed states are very

small, their overall behaviour is very much similar to that of the pure states. To qualitatively analyse the error due to the imperfect initial state, we calculated the entanglement and discord monogamy scores by applying ideal operations on the experimental initial state and the results are also shown in the Fig. 3. The overall agreement of the experimental results with the theoretically expected ones that consider the experimental initial state is remarkable. By comparing Figs. 3(a) and 3(b), we conclude that the monogamy scores for negativity squared and quantum discord have a similar behaviour in both the frustrated and non-frustrated regimes. This is despite the fact that the two corresponding bipartite quantum correlations are defined through widely different approaches – one is via an entanglement-separability criterion and the other is through an information-theoretic paradigm. As noted before, the behaviour of each one of the multipartite quantum correlation measures is different in the frustrated and non-frustrated regimes. Therefore, the monogamy of quantum correlations turns out to be effective in distinguishing frustrated regimes from non-frustrated ones.

V. CONCLUSION

Quantum correlation of separated quantum systems are known to be useful in a variety of phenomena. However, its detection and quantification remain difficult tasks, specially in a multipartite domain. In this work, we have been able to use quantum correlations to experimentally discern between frustrated and non-frustrated regimes of a triangular arrangement of quantum spins, in a nuclear magnetic resonance system. To attain this goal, we have used the behavior of multipartite quantum correlation measures of the ground states of this system. These multipartite measures are obtained by using the concept of monogamy of quantum correlations, which puts constraints on the sharability of quantum correlations. We believe the present study to be important not only for understanding quantum correlations in general but also in analysing various quantum phase transitions in many-body quantum systems, in particular frustrated quantum systems.

ACKNOWLEDGEMENTS

We thank S. S. Roy for technical help. The use of AV500 FTNMR spectrometers of the NMR Research Centres at IISc, Bangalore and IISER, Pune, and funding by the Department of Science and Technology, New Delhi, are gratefully acknowledged. This work was partly

supported by the DST Projects IR/S2/PU-01/2008 and SR/S2/LOP-0017/2009.

APPENDIX

The negativity N_{12} and the quantum discord D_{12} measured from the experimental states in both the frustrated and non-frustrated regimes are shown in the Fig. 4. The theoretically expected ones are also shown. In both the regimes, both N_{12} and D_{12} increases sharply in the interval $|J|/h=0$ to 1. However, for higher values of $|J|/h$, both the measures saturate in the frustrated regime, whereas they gradually decrease to zero in the non-frustrated one.

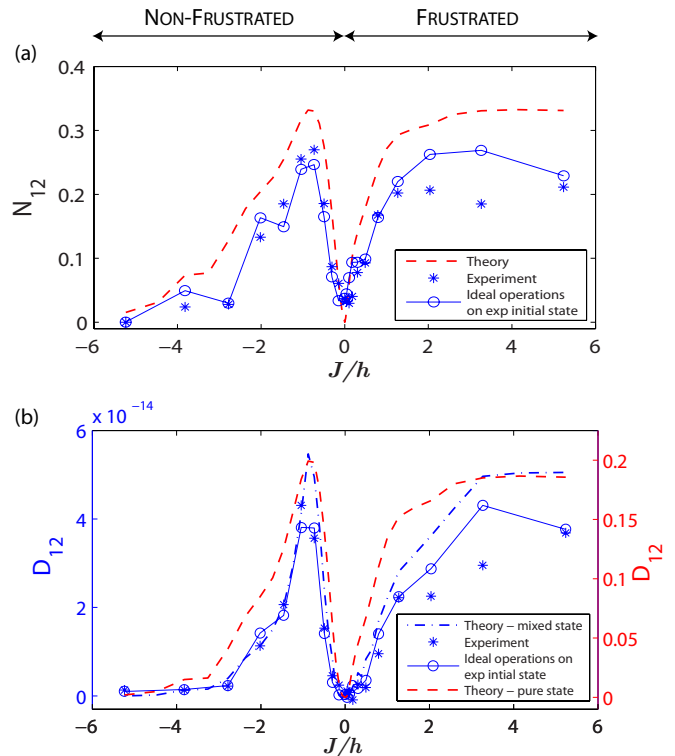


FIG. 4. Bipartite quantum correlations. We plot the negativity, N_{12} , in (a) and the quantum discord, D_{12} , in (b). The red-dashed curves correspond to the theoretically expected results, obtained by applying ideal unitary operations on the ideal initial state. The blue circles are obtained by applying the ideal unitary operations on the experimental initial state. The blue stars correspond to the experimental results. In (b) the experimental results are calculated using the full mixed state density matrices of the NMR system and blue dash-dotted curve represent the theoretically expected results for the same, and the y-axis for the red-dashed curve is given at the right.

[1] R. Horodecki, P. Horodecki, M. Horodecki, and K. Horodecki, Rev. Mod. Phys. **81**, 865 (2009).

[2] K. Modi, A. Brodutch, H. Cable, T. Paterek, and V. Vedral, Rev. Mod. Phys. **84**, 1655 (2012).

- [3] M. Lewenstein, A. Sanpera, V. Ahufinger, B. Damski, A. Sen(De), and U. Sen, *Adv. in Phys.* **56**, 243 (2007).
- [4] L. Amico, R. Fazio, A. Osterloh, and V. Vedral, *Rev. Mod. Phys.* **80**, 517 (2008).
- [5] J.J. Binney, N.J. Dowrick, A.J. Fisher, M.E.J. Newman, *The Theory of Critical Phenomena: An Introduction to the Renormalization Group* (Oxford University Press, Oxford (1998)); S. Sachdev, *Quantum Phase Transitions* (Cambridge University Press, Cambridge, (1999)).
- [6] K. Binder and A.P. Young, *Rev. Mod. Phys.* **58**, 801 (1986); D. Chowdhury, *Spin Glasses and other Frustrated Systems*, (Wiley, New York (1986)); M. Mézard, G. Parisi, and M.A. Virasoro, *Spin Glass Theory and Beyond* (World Scientific, Singapore (1987)); A. Auerbach, *Interacting Electrons and Quantum magnetism*, (Springer, New York (1994)); S. Sachdev, *Quantum Phase Transitions*, (Cambridge University Press, Cambridge (1999));
- [7] M. Rasolt and Z. Tesanović, *Rev. Mod. Phys.* **64**, 709 (1992); M. Sigrist and T.M. Rice, *ibid.* **67**, 503 (1995); R. Melzi, P. Carretta, A. Lascialfari, M. Mambri, M. Troyer, P. Millet, and F. Mila, *Phys. Rev. Lett.* **85**, 1318 (2000). G. Misguich and C. Lhuillier, in *Frustrated spin systems*, edited by H.T. Diep (World Scientific, Singapore (2004)); C. Lhuillier, arXiv:cond-mat/0502464; F. Alet, A.M. Walczak, M.P.A. Fisher, *Physica (Amsterdam)* **369A**, 122 (2006).
- [8] A. Sen(De), U. Sen, J. Dziarmaga, A. Sanpera, and M. Lewenstein, *Phys. Rev. Lett.* **101**, 187202 (2008).
- [9] S.M. Giampaolo, G. Gualdi, A. Monras, and F. Illuminati, *Phys. Rev. Lett.* **107**, 260602 (2011).
- [10] J. Struck, C. Olschlager, R. Le Targat, P. Soltan-Panahi, A. Eckardt, M. Lewenstein, P. Windpassinger, and K. Sengstock, *Science* **333**, 996 (2011); J. Simon, W. S. Bakr, R. Ma, M. E. Tai, P. M. Preiss, and M. Greiner, *Nature (London)* **472**, 307 (2011).
- [11] K. Kim, M.-S. Chang, S. Korenblit, R. Islam, E. E. Edwards, J. K. Freericks, G.-D. Lin, L.-M. Duan, and C. Monroe, *Nature (London)* **465**, 590 (2010).
- [12] J. Zhang, M.-H. Yung, R. Laflamme, A. Aspuru-Guzik, J. Baugh, *Nature Communications* **3**, 880 (2012).
- [13] A.K. Ekert, *Phys. Rev. Lett.* **67**, 661 (1991).
- [14] C.H. Bennett, H.J. Bernstein, S. Popescu, and B. Schumacher, *Phys. Rev. A* **53**, 2046 (1996).
- [15] V. Coffman, J. Kundu, and W.K. Wootters, *Phys. Rev. A* **61**, 052306 (2000).
- [16] B.K. Chakrabarti, A. Dutta, and P. Sen, *Quantum Ising Phases and Transitions in Transverse Ising Model* (Springer, Berlin (1996)).
- [17] M. Koashi and A. Winter, *Phys. Rev. A* **69**, 022309 (2004); T.J. Osborne and F. Verstraete, *Phys. Rev. Lett.* **96**, 220503 (2006); G. Adesso, A. Serafini, and F. Illuminati, *Phys. Rev. A* **73**, 032345 (2006); T. Hiroshima, G. Adesso, and F. Illuminati, *Phys. Rev. Lett.* **98**, 050503 (2007); Y.-C. Ou and H. Fan, *Phys. Rev. A* **75**, 062308 (2007); M. Seevinck, *ibid.* **76**, 012106 (2007); S. Lee and J. Park, *ibid.* **79**, 054309 (2009); A. Kay, D. Kaszlikowski, and R. Ramanathan, *Phys. Rev. Lett.* **103**, 050501 (2009); F.F. Fanchini, M.F. Cornelio, M.C. de Oliveira, and A.O. Caldeira, *Phys. Rev. A* **84**, 012313 (2011); M. Hayashi and L. Chen, *ibid.* **84**, 012325 (2011); F.F. Fanchini, M.C. de Oliveira, L.K. Castelano, and M.F. Cornelio, *Phys. Rev. A* **87**, 032317 (2013), and references therein.
- [18] G. Vidal and R.F. Werner, *Phys. Rev. A*, **65**, 032314 (2002).
- [19] L. Henderson and V. Vedral, *J. Phys. A* **34**, 6899 (2001); H. Ollivier and W. H. Zurek, *Phys. Rev. Lett.* **88**, 017901 (2001).
- [20] R. Prabhu, A.K. Pati, A. Sen(De), and U. Sen, *Phys. Rev. A* **85**(R), 040102 (2012); G.L. Giorgi, *Phys. Rev. A* **84**, 054301 (2011); A. Sen(De) and U. Sen, *Phys. Rev. A* **85**, 052103 (2012); R. Prabhu, A.K. Pati, A. Sen(De), and U. Sen, *Phys. Rev. A* **86**, 052337 (2012); X.-J. Ren and H. Fan, arXiv:1111.5163; A. Streltsov, G. Adesso, M. Piani, and D. Bruß, *Phys. Rev. Lett.* **109**, 050503 (2012); Y.-K. Bai, N. Zhang, M.-Y. Ye, and Z.D. Wang, arXiv:1206.2096; Salini K., R. Prabhu, A. Sen(De), and U. Sen, arXiv:1206.4029.
- [21] M.N. Bera, R. Prabhu, A. Sen(De), and U. Sen, *Phys. Rev. A* **86**, 012319 (2012).
- [22] A. Peres, *Phys. Rev. Lett.* **77**, 1413 (1996); M. Horodecki, P. Horodecki, and R. Horodecki, *Phys. Lett. A* **223**, 1 (1996).
- [23] E. Farhi, J. Goldstone, S. Guttmann, and M. Sipser, quant-ph/0001106; M. Steffen, W. van Dam, T. Hogg, G. Breyta, and I. Chuang, *Phys. Rev. Lett.* **90**, 067903 (2003); A. Mitra, A. Ghosh, R. Das, A. Patel, and A. Kumar, *J. Magn. Reson.* **177**, 285 (2005).
- [24] A. Messiah, *Quantum Mechanics*, vol. II (Wiley, New York (1976)).
- [25] R. R. Ernst, G. Bodenhausen, and A. Wokaun, *Principles of Nuclear Magnetic Resonance in one and two dimensions* (Oxford University Press, Oxford (1990)).
- [26] D. G. Cory, A. F. Fahmy, and T. F. Havel, *Proc. Natl. Acad. Sci. USA* **94**, 1634 (1997).
- [27] N. A. Gershenfeld, and I. L. Chuang, *Science* **275**, 350 (1997).
- [28] N. Khaneja, T. Reiss, C. Kehlet, T. Schulte-Herbruggen, and S. J. Glaser, *J. Magn. Reson.* **172**, 296 (2005).
- [29] C. A. Ryan, *Characterization and Control in Large Hilbert Spaces*, Doctoral Thesis, University of Waterloo (2008).
- [30] S. S. Roy, and T. S. Mahesh, *J. Magn. Reson.* **206**, 127 (2010).
- [31] S. L. Braunstein, C. M. Caves, R. Jozsa, N. Linden, S. Popescu, and R. Schack, *Phys. Rev. Lett.* **83**, 1054 (1999).
- [32] D. O. Soares-Pinto, L. C. Celeri, R. Auccaise, F. F. Fanchini, E. R. deAzevedo, J. Maziero, T. J. Bonagamba, and R. M. Serra, *Phys. Rev. A* **81**, 062118 (2010); G. Passante, O. Moussa, D. A. Trottier, and R. Laflamme, *Phys. Rev. A* **84**, 044302 (2011); H. Katiyar, S. S. Roy, T. S. Mahesh, and A. Patel, *Phys. Rev. A* **86**, 012309 (2012).